

1 **Modeling and Analysis of the Car-truck Heterogeneous Traffic Flow Based on Intelligent**  
2 **Driver Model**

3  
4 Da Yang, Ph.D. Candidate  
5 Department of Civil and Environmental Engineering,  
6 University of Wisconsin-Madison,  
7 1415 Engineering Drive, Madison, WI 53706, USA  
8 Phone: 1-608-334-4281  
9 E-mail: [yangd8@gmail.com](mailto:yangd8@gmail.com)

10  
11 Jing Jin, Ph.D., Postdoctoral Fellow  
12 Department of Civil, Architectural, and Environmental Engineering,  
13 The University of Texas-Austin,  
14 1616 Guadalupe St., Ste. 4.202, Austin, TX 78701, USA  
15 Phone: 1-512-232-3124  
16 E-mail: [jjin@austin.utexas.edu](mailto:jjin@austin.utexas.edu)

17  
18 Bin Ran, Ph.D., Professor  
19 Department of Civil & Environmental Engineering,  
20 University of Wisconsin-Madison,  
21 1415 Engineering Drive, Madison, WI 53706, USA  
22 Phone: 1-608-262-0052 Fax: 1-608-262-5199  
23 Email: [bran@wisc.edu](mailto:bran@wisc.edu)

24 and  
25 School of Transportation, Southeast University,  
26 No.2 Si Pai Lou, Nanjing 210096, China

27  
28 Yun Pu, Ph.D., Professor  
29 School of Transportation and Logistics,  
30 No.111 erhuanlubeiyiduan, Chengdu, 610031, China  
31 Email: [ypu@home.swjtu.edu.cn](mailto:ypu@home.swjtu.edu.cn)

32  
33 Fei Yang, Ph.D., Associate Professor  
34 School of Transportation and Logistics,  
35 No.111 erhuanlubeiyiduan, Chengdu, 610031, China  
36 Email: [yangfeitraffic@gmail.com](mailto:yangfeitraffic@gmail.com)

37  
38 Corresponding Author: Da Yang

39  
40 Submitted for Presentation and Publication  
41 To the 92<sup>nd</sup> Transportation Research Board Meeting  
42 Submission Date: Sep. 15<sup>th</sup>, 2012

43  
44 5449 Words + 1 Table + 6 Figures = 7199 Words

1 **ABSTRACT**

2 The traffic flow heterogeneity caused by the different car-following dynamics among the different types  
3 of vehicles has drawn increasing attention recently. This paper explores the characteristics of the four  
4 types of car-truck car-following combinations, car-following-car (CC), car-following-truck (CT), truck-  
5 following-car (TC) and truck-following-truck (TT), and their impacts on traffic flow stability. A  
6 heterogeneous traffic flow model based on Intelligent Driver Model (IDM) is proposed and calibrated  
7 using the Next Generation Simulation (NGSIM) vehicle trajectory data. Based on the calibrated model,  
8 the characteristics of the car-truck heterogeneous traffic flow are evaluated using the linear stability  
9 analysis, fundamental diagrams, and shock wave characteristics. The linear stability analysis identifies  
10 two critical factors that can influence the stability of the car-truck heterogeneous traffic flow: the  
11 stability functions and the proportions of the four types of car-truck combination. Cars and trucks can  
12 both stabilize and destabilize the traffic flow depending on the combination type and the equilibrium  
13 velocity. Fundamental diagrams of car-truck heterogeneous flow are found to be determined by the  
14 distance headways and proportions of the four types of combination. Moreover, the fundamental  
15 diagrams of different car-truck combinations converge to several clusters with the same proportion  
16 difference between the CC and TT combinations. The slowing-down effect of trucks on shock wave  
17 speed in the car-truck heterogeneous traffic flow is also observed in the simulation.

18

19 **KEYWORDS:** CAR AND TRUCK, HETEROGENEOUS TRAFFIC FLOW, INTELLIGENT  
20 DRIVER MODEL, CAR-FOLLOWING COMBINATIONS

## 1 INTRODUCTION

2 Heterogeneity is a key characteristic of real-world traffic flow. Although traffic flow theories and  
 3 models are usually developed first for the homogeneous traffic flow, most of them can be easily  
 4 converted into their heterogeneous forms. However, the difficulty is the lack of sufficient data to  
 5 calibrate and explore the heterogeneous models. With the development of the data collection technology  
 6 in recent years, such as the video-based method and the GPS-based method, traffic information,  
 7 especially individual vehicle dynamics, can be obtained in greater detail. Many researchers have been  
 8 using these new data sources to investigate the characteristics of car-truck heterogeneous traffic flow in  
 9 the past few years. Early researchers focused on investigating the differences between the car and truck  
 10 driving behavior. Huddart and Lafont (1), McDonald et al. (2) and Sayer et al. (3) compared the  
 11 headway differences between these two cases: car-following-car and car-following-truck, but their  
 12 studies did not reach conclusive results regarding with which case had the larger headway. Peeta et al. (4,  
 13 5) analyzed interactions of cars and trucks in multiple lanes. Highway Capacity Manual presented that  
 14 trucks occupied more space, had poorer operating capabilities, and created larger gaps than cars in most of  
 15 situations (6). However, these studies (1-5) did not recognize that the car-following behavior also depends  
 16 on the following vehicle type. Ye's study (7) first explores the impact of the following vehicle type (car  
 17 or truck) on traffic flow. He concluded that the four types of car-truck car-following combination should  
 18 be taken into account in the study of the car-truck heterogeneous traffic flow: the car-following-car (CC),  
 19 the car-following-truck (CT), the truck-following-car (TC), and the truck-following-truck (TT). Sarvi (8)  
 20 also studied the driving behavior of these three car-following combinations, car-following-car, truck-  
 21 following-car and car-following-truck. Aghabayk et al. (9) further studied the distance headway, time  
 22 headway, reaction time and car-following threshold variations among the four types of combination. One  
 23 major limitation of those early studies on car-truck traffic flow characteristics is the lack of modeling of  
 24 the dynamic traffic flow characteristics. Mason and Woods (10) developed the homogeneous Optimal  
 25 Velocity (OV) car-following model into a heterogeneous traffic flow model to describe the interaction  
 26 between cars and trucks. The derived OV heterogeneous car-following model is as follows,

$$27 \quad \frac{d^2 x_n(t)}{dt^2} = \lambda_n (U_n(x_{n-1} - x_n) - v_n) \quad (1)$$

28 where  $x_n(t)$  and  $v_n(t)$  respectively denote the location and velocity of the vehicle  $n$  at time  $t$ ,  $x_{n-1}(t)$   
 29 denotes the location of the vehicle  $n-1$  (the preceding vehicle of vehicle  $n$ ) at time  $t$ ,  $\lambda_n$  denotes the  
 30 sensitivity parameter of the vehicle  $n$ ,  $U_n(x_{n+1} - x_n)$  denotes the optimal velocity function the vehicle  $n$   
 31 wishes to take, and it is the function of the headway of vehicle  $n$ .

32 The heterogeneous Optimal Velocity model is used to conduct the comparison of the car-  
 33 following dynamics between homogeneous and heterogeneous vehicles and it is found that trucks may

dampen congestion waves. Because of the complication in their multi-species formulations, it is difficult to analyze individually how different car-truck following combinations can affect traffic flow. In this study, based on Intelligent Driver Model (IDM), we developed a heterogeneous model with the different sub-models for each car-truck following combination. To calibrate the new model, the model parameters for each car-truck car-following combination are calibrated separately using the car-following data extracted from the I-80 NGSIM (Next Generation Simulation) data for each combination. Based on the calibrated model, we study the three characteristics of the car-truck heterogeneous traffic flow, the linear stability, fundamental diagrams, and shock wave.

## METHODOLOGY

### An IDM-based Car-following Model for the Car-truck Heterogeneous Traffic Flow

Treiber et al. proposed Intelligent Driver Model in 2000 (11) for the homogeneous traffic flow. This model is a widely explored car-following model (12-14), and its formulation is as follows,

$$\begin{cases} \frac{d^2 x_n(t)}{dt^2} = a \left[ 1 - \left( \frac{v_n(t)}{V} \right)^\delta - \left( \frac{S(v_n(t), \Delta v_n(t))}{\Delta x_n(t) - l} \right)^2 \right] \\ S(v_n(t), \Delta v_n(t)) = s^0 + s^1 \sqrt{\frac{v_n(t)}{V}} + \tau v_n(t) - \frac{v_n(t) \cdot \Delta v_n(t)}{2\sqrt{ab}} \end{cases} \quad (2)$$

where  $a$  is the maximum acceleration,  $V$  is the desired velocity,  $\delta$  is the acceleration exponent,  $S(\cdot)$  is the desired minimum gap,  $s^0$  and  $s^1$  are the jam distances,  $\tau$  is the safe time headway,  $b$  is the desired deceleration,  $l$  is the leading vehicle length, and  $\Delta v_n(t) = v_{n-1}(t) - v_n(t)$  is the removal rate of the vehicle  $n$  to its preceding vehicle  $n-1$ .

We develop the homogeneous IDM to its heterogeneous form by giving subscripts to the model parameters. The proposed heterogeneous IDM formulates the four different car-truck car-following combinations as follows,

$$\begin{cases} \frac{d^2 x_n(t)}{dt^2} = a_n \left[ 1 - \left( \frac{v_n(t)}{V_n} \right)^{\delta_n} - \left( \frac{S_n(v_n(t), \Delta v_n(t))}{\Delta x_n(t) - l_n} \right)^2 \right] \\ S_n(v_n(t), \Delta v_n(t)) = s_n^0 + s_n^1 \sqrt{\frac{v_n(t)}{V_n}} + \tau_n v_n(t) - \frac{v_n(t) \cdot \Delta v_n(t)}{2\sqrt{a_n b_n}} \end{cases} \quad (3)$$

where all the parameters  $a_n$ ,  $\delta_n$ ,  $V_n$ ,  $s_n^0$ ,  $s_n^1$ ,  $\tau_n$  and  $b_n$  have four alternatives. Taking  $a_n$  as an example,  $a_n$  can be  $a_{cc}$ ,  $a_{ct}$ ,  $a_{tc}$  and  $a_{tt}$ . The leading vehicle length  $l$  has two alternatives,  $l_c$  and  $l_t$ .

In the homogeneous traffic flow, all vehicles at the equilibrium state have zero acceleration, the same distance headway and the same velocity; while at the equilibrium state, all vehicles in the

1 heterogeneous traffic flow still have zero acceleration and the same velocity, but their distance headways  
 2 vary for different vehicles which can be described using the following equations:

$$3 \quad v_n = v^*, \dot{v}_n = 0, \text{ and } h_n = h_n^* \quad (4)$$

4 where  $v^*$  is the equilibrium velocity which is the same for all vehicles,  $h_n^*$  is the corresponding  
 5 equilibrium headway of the vehicle  $n$ , and  $h_n^*$  varies among the vehicles. Substituting (4) into the  
 6 heterogeneous IDM (3) yields,

$$7 \quad \begin{cases} 1 - \left(\frac{v^*}{v_0}\right)^\delta - \left(\frac{\hat{s}(v^*, 0)}{h_{IDM}^* - l}\right)^2 = 0 \\ \hat{s}(v^*, 0) = s^0 + s^1 \sqrt{v^*/v_0} + \tau v^* \end{cases} \quad (5)$$

8 Rewriting the above equation yields,

$$9 \quad h^* = \frac{s_0 + s_1 \sqrt{v^*/v_0} + \tau v^*}{\sqrt{1 - (v^*/v_0)^\delta}} + l \quad (6)$$

10 In the car-truck heterogeneous flow,  $h^*$  has the four alternatives,  $h_{cc}^*$ ,  $h_{ct}^*$ ,  $h_{tc}^*$  and  $h_{tt}^*$  which  
 11 correspond to the four types of combinations. It should be noticed that the vehicle length  $l$  in  $h^*$  only  
 12 depends on the leading vehicle type, namely,  $l = l_c$  in  $h_{cc}^*$  and  $h_{tc}^*$ , and  $l = l_t$  in  $h_{ct}^*$  and  $h_{tt}^*$ .

13 Then, the fundamental diagram of the heterogeneous IDM for the equilibrium state can be  
 14 derived based on Equation (6). Assume a given heterogeneous traffic flow on a single lane contains  $N$   
 15 vehicles. The length of the entire traffic flow in the equilibrium state is:

$$16 \quad L_{total} = \sum_{n=1}^N h_n^* \quad (7)$$

17 In the car-truck heterogeneous traffic flow,  $L_{total}$  has the following formula:

$$18 \quad L_{total} = N_{cc} h_{cc}^* + N_{ct} h_{ct}^* + N_{tc} h_{tc}^* + N_{tt} h_{tt}^* \quad (8)$$

19 where  $N_{cc}$ ,  $N_{ct}$ ,  $N_{tc}$  and  $N_{tt}$  are the numbers of the CC, CT, TC and TT combinations in the car-truck  
 20 heterogeneous traffic flow. Hence, the density of traffic flow can be calculated as:

$$21 \quad k = \frac{N}{N_{cc} h_{cc}^* + N_{ct} h_{ct}^* + N_{tc} h_{tc}^* + N_{tt} h_{tt}^*} \quad (9)$$

22 Rewriting equation (9) in the following form:

$$23 \quad k = \frac{1}{P_{cc} h_{cc}^* + P_{ct} h_{ct}^* + P_{tc} h_{tc}^* + P_{tt} h_{tt}^*} \quad (10)$$

24 where  $P_{cc}$ ,  $P_{ct}$ ,  $P_{tc}$  and  $P_{tt}$  are the proportions of the CC, CT, TC and TT combinations. Thus, the  
 25 fundamental diagram of the car-truck heterogeneous traffic flow has the following relationship:

$$q = \frac{v^*}{P_{cc}h_{cc}^* + P_{ct}h_{ct}^* + P_{tc}h_{tc}^* + P_{tt}h_{tt}^*} \quad (11)$$

where  $q$  is the flow rate of the car-truck heterogeneous traffic flow in space.

Equation (11) indicates that the distance headways and proportions of the four types of combination determine the fundamental diagram of the car-truck heterogeneous traffic flow.

5

### 6 Linear Stability Criterion of the Car-truck Heterogeneous Traffic Flow

7 The linear stability analysis investigates the perturbation propagation characteristic of a vehicle platoon  
8 by adding a small perturbation on the first vehicle of the platoon (13, 15). The stability criterion of IDM  
9 can be derived by following the general stability criterion summarized by Wilson and Ward (13). The  
10 derivation of the detailed stability criteria of IDM requires the partial differentials of the velocity,  
11 headway and velocity difference between the leading and following vehicles with respect to the  
12 equilibrium state of IDM.

$$f_v = -a\delta\left(\frac{v^*}{V}\right)^{\delta-1} - \frac{2aS^*}{(h^*-l)^2}S_v, \quad f_{\Delta v} = -\frac{2aS^*}{(h^*-l)^2}S_{\Delta v}, \quad f_h = 2a(S^*)^2(h^*-l)^3 \quad (12)$$

14 where  $S^* = S(v^*, 0, h^*)$ .  $S_v$ ,  $S_{\Delta v}$  and  $S_h$  are respectively the partial differences of the desired minimum  
15 gap function with respect to the  $v_n$ ,  $\Delta v_n$  and  $\Delta x_n$  at the equilibrium state  $(v^*, 0, h^*)$ . Hence, according to  
16 the general stability criterion introduced by Wilson and Ward (13), the stability criterion of IDM is as  
17 follows,

$$f_{\Delta v}f_v + f_h - \frac{f_v^2}{2} < 0 \quad (13)$$

19 Substituting equation (12) into (13) yields the stability criterion of IDM,

$$\frac{2(S^*)^2}{(h^*-l)^3} + \frac{2aS^*S_{\Delta v}}{(h^*-l)^2} \left( \delta\left(\frac{v^*}{v_0}\right)^{\delta-1} + \frac{2S_vS^*}{(h^*-l)^2} \right) - \frac{a}{2} \left( \delta\left(\frac{v^*}{v_0}\right)^{\delta-1} + \frac{2S^*}{(h^*-l)^2} \right)^2 < 0 \quad (14)$$

21 The derivation of the linear stability criterion of the car-truck heterogeneous traffic is more  
22 complicated. Ward (16) presented the general formula of the linear stability criterion of the  
23 heterogeneous traffic flow as follows,

$$\sum_n \left[ (f_{n,\Delta v} \cdot f_{n,v} + f_{n,h} - f_{n,v}^2/2) \cdot \left( \prod_{j \neq n} f_{j,h} \right)^2 \right] < 0 \quad (15)$$

1 where  $f_{n,v}$ ,  $f_{n,\Delta v}$ ,  $f_{n,h}$  are the partial differences of the car-following model adopted by the vehicle  $n$   
 2 with respect to  $v$ ,  $\Delta v$  and  $\Delta x$  at the equilibrium state where  $v_n = v^*$ ,  $\Delta v_n = 0$  and  $\Delta x_n = h_n^*$ .

3 However, Equation (15) cannot directly reflect the proportion information of the different  
 4 combinations, so we rewrite it as the following form using the induction method:

$$5 \quad \sum_{i=1}^Q \left[ NP_i (f_{i,\Delta v} \cdot f_{i,v} + f_{i,h} - f_{i,v}^2 / 2) \cdot (f_{i,h})^{2NP_i - 2} \prod_{\substack{j \neq i \\ j=1}}^Q (f_{j,h})^{2NP_j} \right] < 0, \quad (16)$$

6 where  $Q$  is the number of the combinations in a given car-truck heterogeneous traffic flow,  $N$  is the total  
 7 number of vehicles in the traffic flow,  $N_i$  is the total number of the combination type  $i$  in the platoon,

8  $P_i = \frac{N_i}{N}$  is the proportion of the combination type  $i$  in total, and  $\sum_{i=1}^M P_i = 1$ . In the car-truck

9 heterogeneous traffic flow,  $Q = 4$  and  $i$  has four alternatives: CC, CT, TC and TT.

10 Equation (16) can be further simplified as follows,

$$11 \quad \sum_{i=1}^Q \left[ P_i \frac{f_{i,\Delta v} \cdot f_{i,v} + f_{i,h} - f_{i,v}^2 / 2}{f_{i,h}^2} \right] < 0 \quad (17)$$

12 In Equation (17), two parts determine the stability criterion of the car-truck heterogeneous traffic  
 13 flow: the fraction part  $\frac{f_{i,\Delta v} \cdot f_{i,v} + f_{i,h} - f_{i,v}^2 / 2}{f_{i,h}^2}$  providing the stability characteristic of the combination  
 14  $i$  and the proportion part  $P_i$  of the combination  $i$ . We define the fraction part as the Stability Function  
 15 ( $SF$ ) of the combination,

$$16 \quad SF_i(f_{i,v}, f_{i,\Delta v}, f_{i,h}) = \frac{f_{i,\Delta v} \cdot f_{i,v} + f_{i,h} - f_{i,v}^2 / 2}{f_{i,h}^2} \quad (18)$$

17 where  $SF_i$  is the stability function of the combination type  $i$ . In addition, comparing the stability criterion  
 18 of IDM (14) with equation (18), it can be found that  $SF$  has the same sign as (14), so  $SF$  also can be used  
 19 to judge the stability of the car-following combination  $i$ . The stability effects of combination type  $i$   
 20 denoted as  $SF_i$  in the car-truck heterogeneous traffic flow can be written as follows,

$$21 \quad SF_i = \frac{(h_i^* - l_i)^6}{4a_i^2 (S_i^*)^4} \cdot \left[ \frac{2(S_i^*)^2}{(h_i^* - l_i)^3} + \frac{2a_i S_i^* S_{i,\Delta v}}{(h_i^* - l_i)^2} \left( \delta_i \left( \frac{v^*}{V_i} \right)^{\delta_i - 1} + \frac{2S_{i,v} S_i^*}{(h_i^* - l_i)^2} \right) - \frac{a_i}{2} \left( \delta_i \left( \frac{v^*}{V_i} \right)^{\delta_i - 1} + \frac{2S_i^*}{(h_i^* - l_i)^2} \right)^2 \right] \quad (19)$$

22 Moreover, we define the left part of equation (17) as the stability function  $F$  of the car-truck  
 23 heterogeneous traffic flow. Thus, in the car-truck heterogeneous traffic flow, there is,

$$24 \quad F = P_{cc} \cdot SF_{cc} + P_{ct} \cdot SF_{ct} + P_{tc} \cdot SF_{tc} + P_{tt} \cdot SF_{tt} \quad (20)$$

1           When  $F < 0$ , the car-truck heterogeneous traffic flow is stable. Equation (20) indicates that the  
 2 proportion of the car and the truck is not the only deciding factor of the stability of heterogeneous traffic  
 3 flow, and the stability function of each car-truck following combination is also significant. Furthermore,  
 4 on a ring road, the stability function of the car-truck heterogeneous traffic flow and the proportions of  
 5 four types of combination have the following relationship:

$$6 \quad \begin{cases} F_l = P_{cc} \cdot SC_{cc} + P_{ct} \cdot SC_{ct} + P_{tc} \cdot SC_{tc} + P_{tt} \cdot SC_{tt} \\ P_{cc} + P_{ct} + P_{tc} + P_{tt} = 1 \\ P_{ct} = P_{tc} \end{cases} \quad (21)$$

7

### 8 **Model Calibration and Experimental Design**

9 The car-following model calibration is a nonlinear optimization problem. In this study, we use Genetic  
 10 Algorithm (GA) to solve this nonlinear optimization problem to obtain the optimal parameters. We also  
 11 adopt the Theil's  $U$  function as the objective function as suggested in several existing studies (17, 18).

$$12 \quad F_{objective} = \frac{\sqrt{\frac{1}{M} \sum_{m=1}^M (y_m^{real} - y_m^{sim})^2}}{\sqrt{\frac{1}{M} \sum_{m=1}^M (y_m^{real})^2} + \sqrt{\frac{1}{M} \sum_{m=1}^M (y_m^{sim})^2}} \quad (22)$$

13 where  $y_m^{real}$  is the real data,  $y_m^{sim}$  is the simulation result from the model, and  $m=1, \dots, M$  is the number  
 14 of the data sample.

15 To calibrate car-following models, we use the NGSIM vehicle trajectory data collected on I-80  
 16 San Francisco, California on April 13, 2005 (19). Since the data includes lane change and large vehicle  
 17 gaps, we use the following criteria to extract the car-following datasets of the four combinations  
 18 separately from NGSIM data.

- 19 a. Each car-following group contains two vehicles (car-following pair). Car-following group  
 20 with more than three vehicles will be divided into multiple two-vehicle groups.
- 21 b. Each pair of car-following vehicles is formed and decomposed based on two spacing  
 22 thresholds, the engaging threshold  $DE = 130$  ft (39.62 m) and the disengaging threshold  $DD$   
 23  $= 150$  ft (45.72 m). These values are determined based on critical density at the experimental  
 24 site. Using two thresholds instead of one threshold can avoid unnecessary frequent grouping  
 25 and ungroup of car-following vehicle pairs caused by small fluctuation of spacing value  
 26 around a single threshold.
- 27 c. If a vehicle group decomposes due to spacing increase, lane changing or reaching the end of  
 28 the segment, it will not be exported as a valid sample.



1           The final datasets include the 477712, 25844, 16471, and 10105 trajectory points for the CC, CT,  
 2 TC, and TT combinations respectively. The calibrated car-following models are also inspected using  
 3 several error indexes including Mean Error (ME), Mean Absolute Error (MAE) and Mean Absolute  
 4 Relative Error (MARE) as follows,

$$5 \quad ME = \frac{\sum_{m=1}^M (y_m^{real} - y_m^{sim})}{M} \quad (23)$$

$$6 \quad MAE = \frac{\sum_{m=1}^M |y_m^{real} - y_m^{sim}|}{M} \quad (24)$$

$$7 \quad MARE = \frac{\sum_{m=1}^M (|y_m^{real} - y_m^{sim}| / y_m^{real})}{M} \quad (25)$$

8 where  $m$  indicates the  $m^{\text{th}}$  sample,  $M$  is the total number of samples,  $y_m^{real}$  is the  $m^{\text{th}}$  real data sample ( $y$   
 9 can be the acceleration, velocity or position), and  $y_m^{sim}$  is the  $m^{\text{th}}$  simulation data sample.

10           To investigate the stability and characteristics of the car-truck heterogeneous traffic flow, a ring-  
 11 road numerical simulation is conducted by placing 100 vehicles on a single-lane, flat, and ring road, with  
 12 the first vehicle following the end vehicle. In the simulations, the initial state of the traffic flow is  
 13 equilibrium state, add a small perturbation on the first vehicle, and then observe the perturbation  
 14 development in the platoon. Many studies adopted this simulation method to explore the fundamental  
 15 diagram (20, 21), shock wave (21, 22), linear stability (13, 23), and other properties (24) of traffic flow.

16

## 17 **RESULTS ANALYSIS**

### 18 **Preliminary Data Analysis**

19 Some preliminary analysis is conducted to obtain the general characteristics of the different car-truck  
 20 car-following combination types. First, the gap versus velocity relationship for each combination type is  
 21 explored. The CC combination has the smallest average gap, and the TT combination has the largest  
 22 average gap for the same velocity. When  $v = 17$  m/s, the CT combination has the same gap with the TC  
 23 combination. The CT combination has a larger gap than the TC combination before  $v = 17$  m/s, while the  
 24 TC combination has a larger gap after  $v = 17$  m/s. Second, the desired velocities of cars and trucks are  
 25 also studied. The statistical results show that the truck has the maximum velocity 18 m/s, and the car has  
 26 the maximum velocity 30 m/s. The maximum velocity of the CT combination is around 18m/s which is  
 27 restricted by the maximum velocity of the leading truck. The maximum velocity found for the CT  
 28 combination is around 23 m/s with the combined impacts of the slow-moving follower truck and fast-

1 moving leader car. The CC and TT combinations respectively had the maximum velocities of 30 m/s and  
 2 16 m/s. Third, the significant difference in response time for the different vehicle types suggested by (25)  
 3 can be measured using the method introduced by Aghabayk et al. (9). The average response time of the  
 4 truck drivers is found to be 2.1 s, and the average response time of the car drivers is around 1.3 s.

### 5 Calibration and Evaluation Results

6 Table 1 lists the calibration results of the heterogeneous IDM. The calibrated desired velocities of the  
 7 four combinations are similar to the preliminary statistical results. The TT combination has the largest  
 8 jam spaces ( $s_n^0$  and  $s_n^1$ ); while the CC combination has the smallest jam spaces. The order of the safe  
 9 time headway  $\tau_n$  is  $CC < CT < TC < TT$ . Cars have larger deceleration  $b_n$  than trucks. The acceleration  
 10 exponents are same for all four types of combination. The values of the error indexes of acceleration,  
 11 velocity, and location for each combination type can also be found in Table 1. The acceleration  
 12 simulation errors (MARE) for the four combinations are all less than 15%, and the velocity and location  
 13 simulation errors (MARE) are all less than 10%. Therefore, the calibration results can reflect the car-  
 14 following behavior characteristics of the four combinations in the I-80 NGSIM vehicle trajectory data.

15 **TABLE 1 Calibration and evaluation results of the four combinations**

	Variables	CC	CT	TC	TT
Calibration Results	$a_n$ (m/s <sup>2</sup> )	1.01	1.03	0.78	0.74
	$V_n$ (m/s)	27	19.3	20.6	17.7
	$s_n^0$ (m)	0.85	1.35	1.11	1.53
	$s_n^1$ (m)	0.19	0.27	0.12	0.36
	$\tau_n$ (s)	1.2	1.4	1.8	2.0
	$b_n$ (m/s <sup>2</sup> )	2.26	2.12	1.70	1.61
	$\delta_n$	4	4	4	4
Acceleration Evaluation	ME	0.84	0.28	-0.03	0.13
	MAE	1.17	1.67	1.24	1.16
	MARE	0.11	0.13	0.12	0.1
Velocity Evaluation	ME	-0.25	0.15	-0.23	-0.04
	MAE	1.31	1.62	1.2	0.75
	MARE	0.08	0.09	0.07	0.05
Location Evaluation	ME	2.44	3.00	-1.93	1.23
	MAE	9.71	9.6	5.75	5.61
	MARE	0.05	0.06	0.03	0.04

2

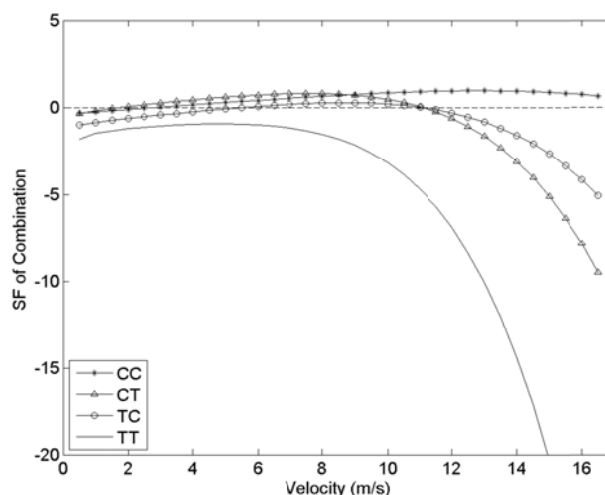
3 **Linear Stability Analysis**

6 The key focus of the linear stability analysis is to investigate the impacts of the two critical factors on the  
 7 stability of the car-truck heterogeneous traffic flow: the individual stability and the proportions of the  
 8 four types of combination.

7 **Individual Stability of the four combinations**

11 The stability function  $SF_i$  for each combination type  $i$  is used to evaluate its individual stability effect on  
 12 the car-truck heterogeneous traffic flow. FIGURE 1 displays the relationship between  $SF$  versus the  
 13 equilibrium velocity for each combination type. The relative order of the  $SF$  for each combination type  
 14 has the following three cases.

- 15 • CT $\approx$ CC>TC>TT. This case happens before  $v^* = 9$  m/s. In this case, the CT combination is the  
 16 most unstable combination and the TT combination is the most stable combination. The CC  
 17 combination effect is close to the CT combination. The truck as the following vehicle is more  
 18 stable than the car as the following vehicle.
- 19 • CC>CT>TC>TT. This case occurs in the middle range of velocity from 9 m/s to 11 m/s, and the  
 20 CC combination becomes the most unstable case. The truck as the leading vehicle in the  
 21 combination is more stable than the car as the leading vehicle, and the truck as the following  
 22 vehicle in the combination is more stable than the car as the following vehicle.
- 22 • CC>TC>CT>TT. This case occurs when the velocity is more than 11 m/s. In this case, the CT  
 23 combination is more stable than the TC combination. The truck as the leading vehicle is more  
 24 stable than the car as the leading vehicle.



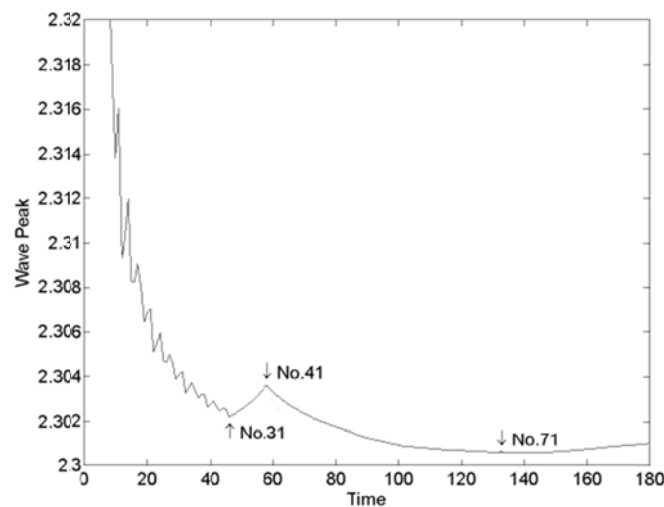
23

24

**FIGURE 1 Stability functions of the four combinations with respect to the uniform velocity.**

5 From the above analysis, the following conclusion can be drawn: the stability effect of cars and  
 6 trucks depends on their leading or following status in car-following and the equilibrium velocity of the  
 7 car-truck heterogeneous traffic flow. This conclusion is more sophisticated than the previous studies (10,  
 8 26) in which the truck or car only has one single effect (stabilize or destabilize) on the traffic flow.

17 In the following ring-road simulation, to demonstrate the different effects of the four  
 18 combinations on traffic flow, we fill the ring road with 30 vehicles alternating between cars and trucks  
 19 followed by 10 cars, 30 trucks and 30 cars. Therefore, the proportions of the CC, CT, TC and TT  
 20 combinations are 39%, 16%, 16% and 29%. Set the equilibrium velocity as 4 m/s. In this case, the  
 21 stability function of the car-truck heterogeneous traffic flow  $F = -0.410$  indicating that the traffic flow is  
 22 stable. The stability functions of the four combinations are  $SF_{cc} = 0.28$ ,  $SF_{ct} = 0.43$ ,  $SF_{tc} = -0.83$ , and  $SF_{tt}$   
 23  $= -1.57$ , which means that the CC and CT combinations can amplify the perturbation, the TC and TT  
 24 combinations will suppress the perturbation, and the car-truck alternating can decrease the perturbation  
 25 ( $SF_{ct} + SF_{tc} < 0$ ). The shock wave peak (See Figure 2) fluctuates and descends at first (the car-truck  
 26 alternating part), ascends after the Vehicle No.31 (the CC combination part), and descends after the  
 27 Vehicle No.41 (the TT combination part), and ascends slightly again after the Vehicle No.71 (the CC  
 28 combination part). Thus, the simulation results are consistent with the analytical analysis.

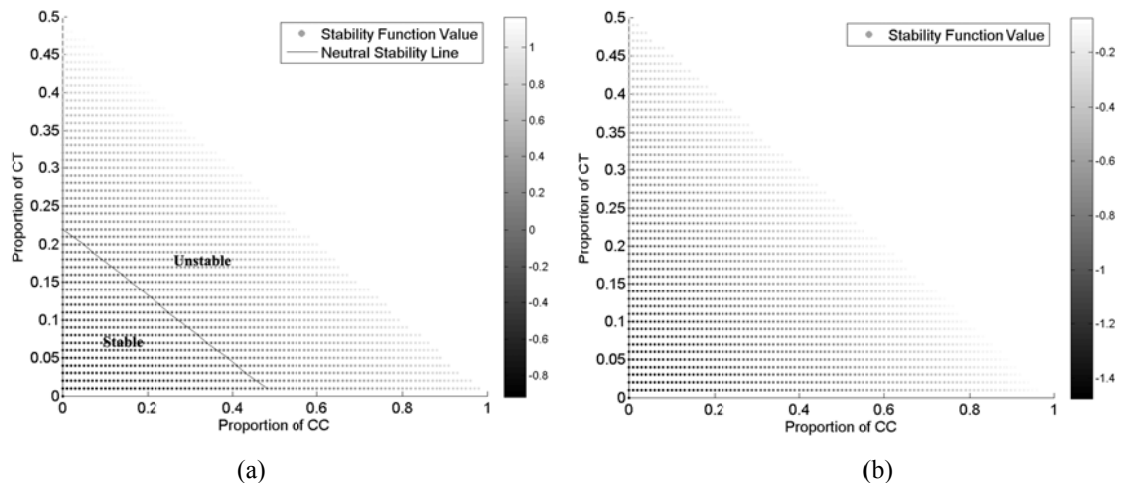


18  
 19 **FIGURE 2 The profile of the shock wave peak.**

20  
 21 ***Impact of the proportions of the four combinations on stability***

25 As shown in Equation (21), the stability function of the car-truck heterogeneous traffic flow is a  
 26 weighted average of the individual values  $SF_{cc}$ ,  $SF_{ct}$ ,  $SF_{tc}$ , and  $SF_{tt}$  according to the proportions of the  
 27 car-truck combination types. Take the case  $v^* = 6$  m/s as an example and find the corresponding  $SF$   
 28 values of the four combinations from FIGURE 1. Figure 3 (a) is the scatter plot of the stability function

11 values of the car-truck heterogeneous traffic in the space of the CC and CT proportions (According to  
 12 Equation (21), the proportions of CC and TT can determine the proportions of CT and TC). The dots in  
 13 FIGURE 3 (a) are the stability function values, and the line is the neutral stability line connecting all the  
 14 zero stability function values. The neutral stability line splits the quadrant into two areas, the unstable  
 15 area above the line and the stable area under the line. (0, 0.22) and (0.5, 0) are the two critical points.  
 16 When the proportion of the CC combination is more than 0.5 or the CT combination is more than 0.22,  
 17 the traffic flow is always unstable regardless of the proportions of the other three combinations.  
 18 However, when  $v^* = 1$  m/s as shown in FIGURE 3 (b), the four  $SF$  are all negative, which means all  
 19 four combinations are stable. Thus, no neutral stability line exists in this case since the overall stability  
 20 function values are always less than zero.



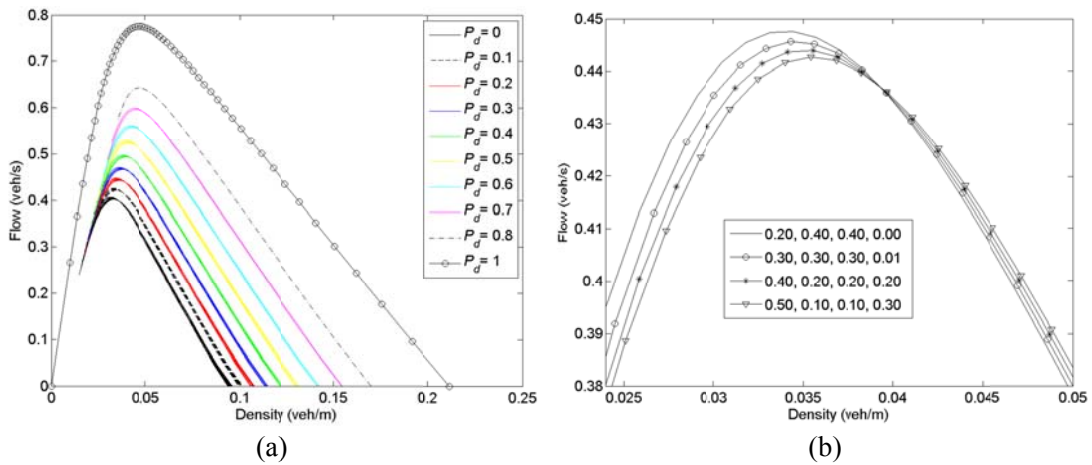
12  
 13  
 15 **FIGURE 3 Scatter plots of the stability function of the car-truck heterogeneous traffic flow. (a)**

16 **The case  $v^* = 1$  m/s. (b) The case  $v^* = 6$  m/s.**

16 **Fundamental Diagram Analysis**

27 We explore the fundamental diagram characteristic of the car-truck heterogeneous traffic flow based on  
 28 equation (11). When examining the fundamental diagram curves for all proportion combinations of the  
 29 CC, CT, TC and TT, we find that the difference between the CC and TT combinations  $P_d = P_{cc} - P_{tt}$  is a  
 30 critical factor to determine the shape and location of the overall fundamental diagram. It is found that  
 31 fundamental diagrams with similar  $P_d$  values locate close to each other on the flow-density plot as  
 32 shown in FIGURE 4 (a). FIGURE 4 (b) illustrates the cluster for the case  $P_d = 0.2$  and the numbers  
 33 beside the legends are the proportions of the four combinations CC, CT, TC and TT respectively. In  
 34 FIGURE 4 (b) the curves have an intersection, and the flow decreases with the increase of  $P_{cc}$  before the  
 35 intersection and increases after the intersection. Furthermore, the flow rate and critical density both  
 36 increase with the increasing of  $P_d$ , which reveals that the most unstable point of the car-truck  
 37 heterogeneous traffic flow moves towards the high flow and high density area with the increasing of  $P_d$ .

3  
4



6 **FIGURE 4 Fundamental diagrams of the car-truck heterogeneous traffic flow. (a) Fundamental**  
7 **diagrams. (b) Fundamental diagram cluster at  $P_d=0.2$ .**

7 **Shock Waves Analysis**

16 The propagation speed of the shock wave is not uniform through the platoon due to the response time  
17 differences between cars and trucks. FIGURE 5 (a) and (b) respectively demonstrate the shock wave  
18 propagations in the pure car traffic flow and the car-truck heterogeneous traffic flow from the trajectory  
19 viewpoint. The arrow indicates the propagation trajectory of a perturbation which gives the shock wave  
20 boundaries between two different states of traffic flow. The slope of the shock wave in the pure car  
21 traffic flow is the same during propagation. However, the slope changes when going through the car-  
22 truck heterogeneous traffic flow and the average slope decreases in the car-truck heterogeneous traffic  
23 flow because the truck needs more time to react to the speed change of its preceding vehicle. Thus, the  
24 shock wave travels faster in the pure car traffic flow than in the car-truck heterogeneous traffic flow.

17  
18  
20  
21

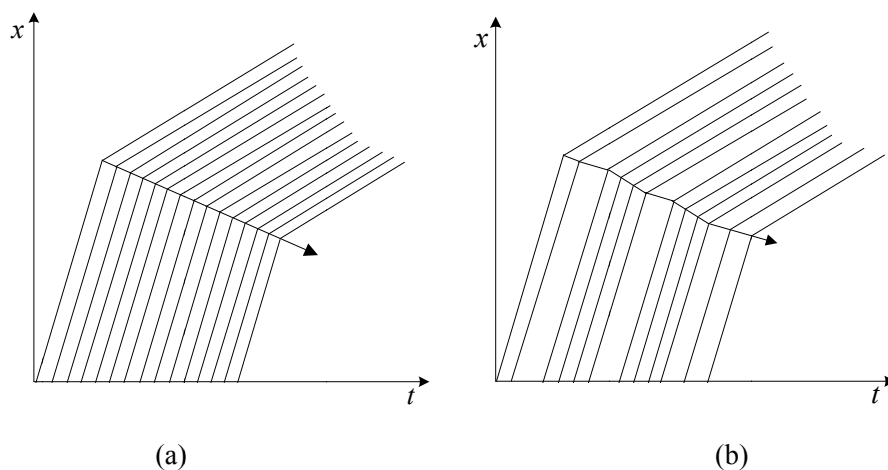
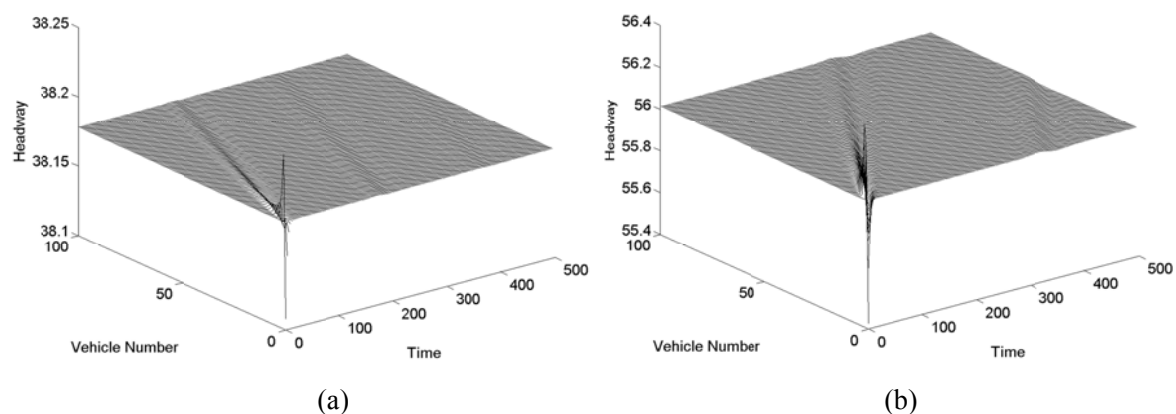


**FIGURE 5 Propagation of the shock wave from the trajectory viewpoint. (a) The pure car traffic**  
**flow. (b) The car-truck heterogeneous traffic flow.**

8           FIGURE 6 illustrates the shock wave propagation observed in a simulation of perturbation  
 9 propagation in both pure car and mixed car-truck flow. The traffic flow in FIGURE 6 (a) is the pure car  
 10 traffic flow, and the traffic flow in FIGURE 6 (b) is the car-truck heterogeneous traffic mixed by 70 cars  
 11 and 30 trucks. Giving the same perturbation to the two types of traffic flow at the same place, the shock  
 12 wave takes around 250 s to propagate to the last vehicle in the pure car traffic flow; while in car-truck  
 13 heterogeneous flow, it takes around 400 s. The simulations illustrate that the car-truck heterogeneous  
 14 traffic flow can slow down the shock wave.



9  
10  
12           **FIGURE 6 Simulation of the propagation speed of the shock wave. (a) The pure car traffic flow.**  
 13   **(b) The car-truck heterogeneous traffic flow.**

## 14 CONCLUSION

23 The traffic flow mixed by cars and trucks is the typical heterogeneous traffic flow in real traffic. In this  
 24 paper, the focus is the analysis of the impacts of the four types of combination, car-following-car (CC),  
 25 car-following-truck (CT), truck-following-car (TC) and truck-following-truck (TT), using heterogeneous  
 26 car-following models. We extend the original Intelligent Driver Model (IDM) to a heterogeneous form  
 27 and use the NGSIM data to calibrate model parameters. The evaluation results show that the calibrated  
 28 car-following models can reflect the car-following dynamics of the four combinations in the car-truck  
 29 heterogeneous traffic flow. Based on the calibrated car-following model, we explore the three  
 30 characteristics of the car-truck heterogeneous traffic flow: the linear stability, fundamental diagrams and  
 31 shock wave.

28           We derive the linear stability criterion of the car-truck heterogeneous traffic flow and validate it  
 29 using the ring-road simulations. Two critical factors, the individual stability function and the proportions  
 30 of the four combinations, are found to determine the stability of the car-truck heterogeneous traffic flow.  
 31 Furthermore, the individual stability function varies with the increasing of equilibrium velocity;  
 32 especially with the increasing of equilibrium velocity, TC becomes less stable than CT. In addition, cars

1 and trucks can both stabilize and destabilize the car-truck heterogeneous traffic flow and their effects  
2 depend on their roles (leading vehicle or following vehicle) in car-following and the equilibrium velocity  
3 of the car-truck heterogeneous traffic flow. This conclusion is more sophisticated than the previous  
4 studies (10, 26) in which the truck or car only has one single effect (stabilize or destabilize) on the traffic  
5 flow. We also investigate the impact of the proportions of the four combination types by simulation. The  
6 results show that the proportions of the four combinations may not have significant influence on the  
7 stability of traffic flow with low equilibrium velocity (e.g. on an extremely congested road); however, in  
8 most cases, the neutral stability lines can be found for the car-truck heterogeneous traffic flow.

9 Fundamental diagrams of the car-truck heterogeneous traffic flow are determined by the  
10 distance headways and the proportions of the four types of combination. The simulations further reveal  
11 that the fundamental diagrams with the same proportion difference between the CC and TT  
12 combinations cluster together. The flow rate and the critical density increase with the increasing of the  
13 proportion difference between the CC and TT. Finally, the shock wave analysis indicates that trucks can  
14 slow down the propagation speed of the shock wave due to their longer response times.

## 16 ACKNOWLEDGMENT

17 This work was supported by the National Natural Science Foundation of China (Grant No.  
18 51278429 and Grant No.50908195) and the National High Technology Research and Development (863)  
19 Program of China (Grant No. 2011AA110403).

## 21 REFERENCES

- 22 1. Huddart K. and R. Lafont. Close driving---Hazard or necessity? In *XV European annual conference*  
23 *on human decision making and manual control*. CD-ROM. TNO, Netherlands, 1990.
- 24 2. McDonald M., M. Brackstone, B. Sultan and C. Roach, Close following on the motorway: initial  
25 findings of an instrumented vehicle study. *VISION IN VEHICLES-VII*, 1999.
- 26 3. Sayer J. R., M. L. Mefford and R. Huang. Ann Arbor. *The effect of lead-vehicle size on driver*  
27 *following behavior*. 2000.
- 28 4. Peeta S., P. Zhang and W. Zhou, Behavior-based analysis of freeway car-truck interactions and related  
29 mitigation strategies. *Transportation Research Part B: Methodological*, Vol.39, No.5, 2005, pp.417-451.
- 30 5. Peeta S., W. Zhou and P. Zhang. Modeling and mitigation of car-truck interactions on freeways. In  
31 *Transportation Research Record: Journal of the Transportation Research Board*, No.1899,  
32 Transportation Research Board of the National Academies, Washington, D.C., 2004, pp.117-126.



- 1 6. TRB. *Highway capacity manual*. Transportation Research Board, National Research Council,  
2 Washington, DC, 2000.
- 3 7. Ye F. and Y. Zhang. Vehicle type-specific headway analysis using freeway traffic data. In  
4 *Transportation Research Record: Journal of the Transportation Research Board*, No.2124,  
5 Transportation Research Board of the National Academies, Washington, D.C., 2009, pp.222-230.
- 6 8. Sarvi M., Heavy commercial vehicles-following behavior and interactions with different vehicle  
7 classes. *Journal of Advanced Transportation*, 2011.
- 8 9. Aghabayk K., M. Sarvi, W. Young and Y. Wang. Investigating heavy vehicle interactions during the  
9 car following process. In *Transportation Research Board 91st Annual Meeting*. CD-ROM.  
10 Transportation Research Board of the National Academies, Washington DC, 2012.
- 11 10. Mason A. D. and A. W. Woods, Car-following model of multispecies systems of road traffic.  
12 *Physical Review E*, Vol.55, No.3, 1997, pp.2203-2214.
- 13 11. Treiber M., A. Hennecke and D. Helbing, Congested traffic states in empirical observations and  
14 microscopic simulations. *Physical Review E*, Vol.62, No.2, 2000, pp.1805-1824.
- 15 12. Treiber M., A. Kesting and D. Helbing, Delays, inaccuracies and anticipation in microscopic traffic  
16 models. *Physica A*, Vol.360, No.1, 2006, pp.71-88.
- 17 13. Wilson R. and J. Ward, Car-following models: fifty years of linear stability analysis—a mathematical  
18 perspective. *Transportation Planning and Technology*, Vol.34, No.1, 2011, pp.3-18.
- 19 14. Hamdar S. H. and H. S. Mahmassani. From existing accident-free car-following models to colliding  
20 vehicles: exploration and assessment. In *Transportation Research Record: Transportation Research*  
21 *Record*, No.2088, Transportation Research Board of the National Academies, Washington, D.C., 2008,  
22 pp.45-56.
- 23 15. Herman R., E. W. Montroll, R. B. Potts and R. W. Rothery, Traffic Dynamics: Analysis of Stability  
24 in Car Following. *Operations Research*, Vol.7, No.1, 1959, pp.86-106.
- 25 16. Ward J. A., Heterogeneity, Lane-Changing and Instability in Traffic: A Mathematical Approach.  
26 *Ph.D. Thesis*. University of Bristol, 2009.
- 27 17. Brockfeld E., R. D. Kühne and P. Wagner. Calibration and validation of microscopic models of  
28 traffic flow. In *Transportation Research Record: Transportation Research Record*, No.1934,  
29 Transportation Research Board of the National Academies, Washington, D.C., 2005, pp.179-187.
- 30 18. Punzo V. and F. Simonelli. Analysis and Comparison of Microscopic Traffic Flow Models with Real  
31 Traffic Microscopic Data. In *Transportation Research Record: Transportation Research Record*,  
32 No.1934, Transportation Research Board of the National Academies, Washington, D.C., 2005, pp.53-63.
- 33 19. *NGSIM data set*. Federal Highway Administration. <http://www.ngsim.fhwa.dot.gov>. Accessed  
34 December 1, 2010.

- 1 20. Kerner B. S. and P. Konhäuser, Structure and parameters of clusters in traffic flow. *Physical Review*  
2 *E*, Vol.50, No.1, 1994, pp.54-83.
- 3 21. Wang J., R. Liu and F. Montgomery. Car-following model for motorway traffic. In *Transportation*  
4 *Research Record: Journal of the Transportation Research Board*, No.1934, Transportation Research  
5 Board of the National Academies, Washington, D.C., 2005, pp.33-42.
- 6 22. Nagatani T., Density waves in traffic flow. *Physical Review E*, Vol.61, No.4, 2000, pp.3564-3570.
- 7 23. Wilson R. E., An analysis of Gipps's car-following model of highway traffic. *IMA journal of applied*  
8 *mathematics*, Vol.66, No.5, 2001, pp.509-537.
- 9 24. Hoogendoorn R. G., S. Hoogendoorn, K. A. Brookhuis and W. Daamen. Anticipation and Hysteresis:  
10 Parameter Value Changes and Model Performance in Simple and Multianticipative Car-Following  
11 Models. In *Transportation Research Board 90th Annual Meeting*. CD-ROM. Transportation Research  
12 Board of the National Academies, Washington DC, 2011.
- 13 25. Rothery R. W.: Traffic Flow Theory. In: *Traffic Flow Theory*. Edited by N. H.Gartner CM, and A. K.  
14 Rathi. Washington.D.C: Transportation Research Board; 1998.
- 15 26. Jin S., D. H. Wang, Z. Y. Huang and P. F. Tao, Visual angle model for car-following theory. *Physica*  
16 *A Statistical Mechanics and its Applications*, Vol.390, 2011, pp.1931-1940.